MATHEMATICAL ENGINEERING TECHNICAL REPORTS

Worst Scenario Detection in Limit Analysis of Trusses against Deficiency of Structural Components

Yoshihiro KANNO

METR 2011–18 June 2011

DEPARTMENT OF MATHEMATICAL INFORMATICS
GRADUATE SCHOOL OF INFORMATION SCIENCE AND TECHNOLOGY
THE UNIVERSITY OF TOKYO
BUNKYO-KU, TOKYO 113-8656, JAPAN

WWW page: http://www.keisu.t.u-tokyo.ac.jp/research/techrep/index.html

Worst Scenario Detection in Limit Analysis of Trusses against Deficiency of Structural Components

Yoshihiro Kanno †

Department of Mathematical Informatics,
University of Tokyo, Tokyo 113-8656, Japan

Abstract

This paper addresses the plastic limit analysis of a truss with some deficient structural components. Given the upper bound for the number of deficient members, we consider uncertainty in the locations of deficient members, i.e., the set of deficient members is not specified in advance. Then we attempt to find the worst scenario of deficiency, in which the limit load factor attains the minimum value. We formulate this combinatorial optimization problem as a mixed integer linear programming problem and solve it by using an algorithm with guaranteed global convergence. The deficient structural components in the worst scenario are regarded as key elements which cause the largest degradation of structural performance. Numerical examples illustrate that key elements, as well as the collapse mode in the worst scenario, depends on the number of deficient structural components.

Keywords

Robustness; Uncertainty; Structural degradation; Structural integrity; Plastic limit analysis; Integer optimization.

1 Introduction

This paper discusses a problem of finding the worst scenario of deficiency of structural components in a truss. Possibilistic (or unknown-but-bounded) models rather than stochastic models are employed to represent the uncertainty in the set of damaged components. The plastic limit load factor of a truss is focused as a mechanical performance. Given the number of possible deficient members, the worst scenario is defined as the set of deficient members with which the limit load factor of the damaged truss attains the minimum value.

For assessing the robustness and/or the redundancy of a structure, it is central to analyze the response of an uncertain structural system. If reliable stochastic information of a structural system is available, then a probabilistic reliability analysis can be performed. In contrast, the worst scenario analysis is applicable to problems without reliable stochastic information, because it requires only bounds for the input data to define the uncertainty in data.

The convex model approach [3] is one of the well known methods for the worst scenario analysis. Optimization of structures under uncertainty was also performed based on the convex model

†Address: Department of Mathematical Informatics, Graduate School of Information Science and Technology, University of Tokyo, Tokyo 113-8656, Japan. E-mail: `kanno@mist.i.u-tokyo.ac.jp`. Phone: +81-3-5841-6906, Fax: +81-3-5841-6886.

approach [10, 29, 33]. Some authors use the term "antioptmization" to mean the worst scenario approach; see, e.g., [7, 30]. This terminology is rather misleading because the worst scenario is defined as the optimal solution of an optimization problem. The interval arithmetic is also regarded as a worst scenario approach developed for error analysis in numerical computation with finite precision calculations [1, 27]. The interval arithmetic has been applied to analyze bounds for the response of structural systems possessing uncertainties; see, e.g., [5, 6, 24, 24, 26, 30] and the references therein. Recently, semidefinite programming has been employed for finding outer ellipsoidal bounds for responses of uncertain structural systems [13, 14, 19, 21]. These semidefinite programming approaches are based on the methodology of robust optimization [4]. The worst scenario problem is defined as the global optimal solution of an optimization problem. When the optimization problem is nonconvex, it is difficult to find the global optimal solution in general. To overcome this difficulty, *mixed integer linear programming* (MILP) approaches have been developed for worst scenario analysis of trusses [12, 20]. For more surveys of worst scenario analysis, see [16, 25].

Redundancy of structures is often evaluated with respect to failure of structural components; see, e.g., [8, 9, 28, 31]. High redundancy often means that the structure suffers only small degradation of performance when one or more structural components fail. For example, for building structures there have been many studies on static and dynamic structural responses in situations that some columns and/or beams fail [11, 18, 23, 28, 32]. In these studies the set of deficient structural components is specified. However, for a real-world structure we cannot know in advance which components will fail. In this paper attention is focused on this uncertainty attribute. That is, we specify only an upper bound for the number of deficient members, and then consider a problem of finding the worst deficient scenario with respect to the degradation of the limit load factor. This worst scenario problem is essentially a combinatorial optimization problem. To ensure that the obtained solution is actually the severest deficient scenario, the worst scenario problem should be solved by using an algorithm with guaranteed convergence to the global optimal solution. This motivates us to propose an MILP reformulation of the worst scenario problem in question. An MILP problem can be solved globally by using a branch-and-cut method, etc., and several commercial and non-commercial software packages are available for this purpose.

The paper is organized as follows. In section 2, we define the uncertainty model in structural deficiency and formulate the worst scenario detection problem. In section 3, we show that this problem can be reformulated as an MILP problem, which can enjoy existing algorithms with guaranteed convergence to the global optimal solution. Two numerical examples are demonstrated in section 4. We conclude in section 5.

A few words regarding our notation: All vectors are assumed to be column vectors. The $(m+n)$-dimensional column vector $(\boldsymbol{a}^{\mathrm{T}}, \boldsymbol{b}^{\mathrm{T}})^{\mathrm{T}}$ consisting of $\boldsymbol{a} \in \mathbb{R}^m$ and $\boldsymbol{b} \in \mathbb{R}^n$ is often written as $(\boldsymbol{a}, \boldsymbol{b})$ for simplicity. For two vectors $\boldsymbol{b} \in \mathbb{R}^n$ and $\boldsymbol{c} \in \mathbb{R}^n$, we write $\boldsymbol{b} \geq \boldsymbol{c}$ if $b_i \geq c_i$ $(i = 1, \dots, n)$. Particularly, $\boldsymbol{b} \geq \boldsymbol{0}$ means $b_i \geq 0$ $(i = 1, \dots, n)$. We use $\mathrm{diag}(\boldsymbol{p})$ to denote the $n \times n$ diagonal matrix with a vector $\boldsymbol{p} \in \mathbb{R}^n$ on its diagonal. For a set $\mathcal{S}$, we use $|\mathcal{S}|$ to denote its cardinality. For example, if $\mathcal{S} = \{1, \dots, m\}$, then $|\mathcal{S}| = m$. We denote by $\mathbb{N}$ the set of natural numbers, i.e., $\mathbb{N} = \{1, 2, \dots\}$.

2 Worst scenario problem

The worst scenario in the limit analysis is defined as the set of missing structural elements with which the limit load factor attains minimum.

2.1 Uncertainty model of structural deficiency

Consider an elastic/perfectly-plastic truss consisting of m members. We denote by d the number of degrees of freedom of displacements. Small deformations are assumed throughout the paper.

For each member i, we use a binary variable t_i to indicate soundness of the member. Specifically, the components of a vector $\boldsymbol{t} \in \{0,1\}^m$ are defined by

$$t_i = \begin{cases} 1 & \text{if member } i \text{ is present,} \\ 0 & \text{if member } i \text{ is absent.} \end{cases} \tag{1}$$

Let $\tilde{\boldsymbol{t}}$ denote the nominal (or the intact) truss. We usually suppose that all members are present in the nominal structure, and hence $\tilde{\boldsymbol{t}} = (1,\dots,1)^{\mathrm{T}}$.

Consider two scenarios of degradation represented by $\boldsymbol{t} \in \{0,1\}^m$ and $\boldsymbol{t}' \in \{0,1\}^m$ ($\boldsymbol{t} \neq \boldsymbol{t}'$). If $\boldsymbol{t} \le \boldsymbol{t}'$, then some members in $\boldsymbol{t}'$ are absent in $\boldsymbol{t}$. Suppose that at most α members are possibly missing from the nominal structure, $\tilde{\boldsymbol{t}}$, due to damage, failure, aging, or fire, etc. The set of all such scenarios is given by

$$\mathcal{T}(\alpha, \tilde{\boldsymbol{t}}) = \{\boldsymbol{t} \in \{0,1\}^m \mid \boldsymbol{t} \le \tilde{\boldsymbol{t}},\ \|\tilde{\boldsymbol{t}} - \boldsymbol{t}\|_1 \le \alpha\}, \quad \alpha \in \{0\} \cup \mathbb{N}, \tag{2}$$

where the L^1-norm of the vector $\tilde{\boldsymbol{t}} - \boldsymbol{t}$ is defined by

$$\|\tilde{\boldsymbol{t}} - \boldsymbol{t}\|_1 = \sum_{i=1}^{m} |\tilde{t}_i - t_i|.$$

Note that we do not consider addition of members to the nominal truss. We call $\mathcal{T}(\alpha, \tilde{\boldsymbol{t}})$ the *uncertainty set* of the structural deficiency. The parameter α, called the *uncertainty parameter*, expresses the level of uncertainty in the following sense:

(i) $\mathcal{T}(0, \tilde{\boldsymbol{t}}) = \{\tilde{\boldsymbol{t}}\}$.

(ii) $\alpha \le \alpha'$ implies $\mathcal{T}(\alpha, \tilde{\boldsymbol{x}}) \subseteq \mathcal{T}(\alpha', \tilde{\boldsymbol{t}})$.

Namely, only the intact scenario is considered at $\alpha = 0$, and the range of possible deficiency scenarios increases as α increases.

Let $\tilde{\boldsymbol{x}} \in \mathbb{R}^m$ denote the vector of member cross-sectional areas in the nominal structure, where $\tilde{x}_i > 0$ ($i = 1,\dots,m$). The true value, denoted $\boldsymbol{x}$, is uncertain and is written as

$$\boldsymbol{x} = \mathrm{diag}(\tilde{\boldsymbol{x}})\boldsymbol{t}, \tag{3}$$

where $\boldsymbol{t} \in \mathcal{T}(\alpha, \tilde{\boldsymbol{t}})$. Let $\sigma_{\mathrm{y}} > 0$ denote the yield stress. For simplicity, suppose that the yield stresses in tension and compression share the common absolute value. Then, for each $i = 1,\dots,m$, the modulus of the admissible axial force, denoted $q_{\mathrm{y}i}(x_i)$, is given by

$$\begin{aligned} q_{\mathrm{y}i}(x_i) &= \sigma_{\mathrm{y}} x_i \\ &= \tilde{q}_{\mathrm{y}i} t_i, \end{aligned} \tag{4}$$

where $\tilde{q}_{\mathrm{y}i} = \sigma_{\mathrm{y}} \tilde{x}_i$ is its nominal value.

2.2 Nominal problem in limit analysis

Let $\boldsymbol{q} \in \mathbb{R}^m$ denote the vector of member axial forces. The yield conditions are given by

$$|q_i| - q_{\mathrm{y}i}(x_i) \leq 0, \quad i = 1, \dots, m. \tag{5}$$

Suppose that the external load consists of a constant part, denoted $\boldsymbol{p}_{\mathrm{d}}$, and a proportionally increasing part, represented by $\lambda \boldsymbol{p}_{\mathrm{r}}$. The constant vectors $\boldsymbol{p}_{\mathrm{d}} \in \mathbb{R}^d$ and $\boldsymbol{p}_{\mathrm{r}} \in \mathbb{R}^d \setminus \{\boldsymbol{0}\}$ are sometimes called the *dead load* and the *reference load*, respectively. The parameter $\lambda \in \mathbb{R}$ is called the *load factor*. The force-balance equation is written as

$$H\boldsymbol{q} = \boldsymbol{p}_{\mathrm{d}} + \lambda \boldsymbol{p}_{\mathrm{r}}, \tag{6}$$

where $H \in \mathbb{R}^{d \times m}$ is the equilibrium matrix.

From the lower bound principle, the limit load factor, denoted $\lambda^*(\boldsymbol{x})$, is defined as the maximum value of λ under the constraints in (5) and (6). Precisely, $\lambda^*(\boldsymbol{x})$ is the optimal value of the following problem:

$$\begin{aligned} \max_{\lambda, \boldsymbol{q}} \quad & \lambda && \text{(7a)} \\ \mathrm{s.\,t.} \quad & H\boldsymbol{q} = \boldsymbol{p}_{\mathrm{d}} + \lambda \boldsymbol{p}_{\mathrm{r}}, && \text{(7b)} \\ & |q_i| \leq q_{\mathrm{y}i}(x_i), \quad i = 1, \dots, m. && \text{(7c)} \end{aligned}$$

This is a *linear programming* (LP) problem in variables λ and $\boldsymbol{q}$.

The problem dual to problem (7) is formulated as

$$\begin{aligned} \min_{\boldsymbol{u}, \boldsymbol{c}} \quad & -\boldsymbol{p}_{\mathrm{d}}^{\mathrm{T}} \boldsymbol{u} + \boldsymbol{q}_{\mathrm{y}}(\boldsymbol{x})^{\mathrm{T}} \boldsymbol{c} && \text{(8a)} \\ \mathrm{s.\,t.} \quad & \boldsymbol{p}_{\mathrm{r}}^{\mathrm{T}} \boldsymbol{u} = 1, && \text{(8b)} \\ & c_i \geq |\boldsymbol{h}_i^{\mathrm{T}} \boldsymbol{u}|, \quad i = 1, \dots, m. && \text{(8c)} \end{aligned}$$

Here, $\boldsymbol{u} \in \mathbb{R}^d$ and $\boldsymbol{c} \in \mathbb{R}^m$ are the variables to be optimized, and $\boldsymbol{h}_i \in \mathbb{R}^d$ is the ith column vector of the equilibrium matrix H in (6), i.e.,

$$H = \left[\boldsymbol{h}_1 \;\middle|\; \boldsymbol{h}_2 \;\middle|\; \cdots \;\middle|\; \boldsymbol{h}_m \right].$$

Problem (8) corresponds to the upper bound principle. Indeed, at the optimal solution, $\boldsymbol{u}$ corresponds to the collapse mode and c_i is the modulus of the (plastic) member elongation.

As is known well, the optimal value of problem (8) coincides with the limit load factor $\lambda^*(\boldsymbol{x})$. This relation is formally stated as follows.

Proposition 2.1. *Suppose that problem* (7) *has a feasible solution. Then both* (7) *and* (8) *have optimal solutions, and their optimal values are the same.*

Proof. Since $c_1, \dots, c_m$ are not bounded above and $\boldsymbol{p}_{\mathrm{r}} \neq \boldsymbol{0}$, problem (8) always has a feasible solution. Then the assertion of this proposition immediately follows from the strong duality of LP. □

Remark 2.2. If the assumption of Proposition 2.1 is not satisfied, then the optimal value of problem (8) is not bounded below. Therefore, we define $\lambda^*(\boldsymbol{x}) = -\infty$ if problem (7) is infeasible. ■

2.3 Definition of worst scenario

In section 2.2, the limit load factor has been introduced as a function of $\boldsymbol{x}$. As seen in (3), $\boldsymbol{x}$ is a function of $\boldsymbol{t}$. Therefore, the limit load factor is considered a function of $\boldsymbol{t}$ as

$$\lambda^*(\boldsymbol{x}(\boldsymbol{t})) = \lambda^*(\mathrm{diag}(\tilde{\boldsymbol{x}})\boldsymbol{t}). \tag{9}$$

Since $\boldsymbol{t}$ is supposed to be uncertain, (9) describes the uncertainty in the limit load factor.

For the given α and $\tilde{\boldsymbol{t}}$, $\boldsymbol{t}$ can possibly take any value in $\mathcal{T}(\alpha, \tilde{\boldsymbol{t}})$ defined by (2). The limit load factor in the worst scenario is then defined as the minimum value of $\lambda^*(\boldsymbol{x}(\boldsymbol{t}))$. Formally, the *worst limit load factor*, denoted $\lambda_{\mathrm{min}}(\alpha, \tilde{\boldsymbol{x}})$, for given α and $\tilde{\boldsymbol{x}}$ is defined by

$$\lambda_{\mathrm{min}}(\alpha, \tilde{\boldsymbol{x}}) = \min_{\boldsymbol{t}} \{\lambda^*(\boldsymbol{x}(\boldsymbol{t})) \mid \boldsymbol{t} \in \mathcal{T}(\alpha, \tilde{\boldsymbol{t}})\}. \tag{10}$$

The worst scenario, denoted $\boldsymbol{t}_{\mathrm{w}}$, is the scenario at which the limit load factor attains the worst limit load factor, i.e.,

$$\boldsymbol{t}_{\mathrm{w}} \in \arg\min_{\boldsymbol{t}} \{\lambda^*(\boldsymbol{x}(\boldsymbol{t})) \mid \boldsymbol{t} \in \mathcal{T}(\alpha, \tilde{\boldsymbol{t}})\}. \tag{11}$$

Remark 2.3. As discussed in Remark 2.2, we let $\lambda^*(\boldsymbol{x}) = -\infty$ if problem (7) is infeasible for a given $\boldsymbol{x}$. Therefore, for given α and $\tilde{\boldsymbol{t}}$, if there exists $\boldsymbol{t}' \in \mathcal{T}(\alpha, \tilde{\boldsymbol{t}})$ satisfying

$$\left\{ (\lambda, \boldsymbol{q}) \,\middle|\, \begin{array}{l} H\boldsymbol{q} = \boldsymbol{p}_{\mathrm{d}} + \lambda \boldsymbol{p}_{\mathrm{r}}, \\ |q_i| \le q_{\mathrm{y}i}(x_i(\boldsymbol{t}'))\ (i = 1, \dots, m) \end{array} \right\} = \emptyset,$$

then $\lambda^*(\boldsymbol{x}(\boldsymbol{t}')) = -\infty$, and hence $\lambda_{\mathrm{min}}(\alpha, \tilde{\boldsymbol{x}}) = -\infty$. ■

Since $\lambda^*(\boldsymbol{x}(\boldsymbol{t}))$ included in (10) is the optimal value of problem (8), the minimization problem on the right-hand side of (10) is equivalently rewritten as

$$\begin{aligned} \min_{\boldsymbol{t}, \boldsymbol{q}_{\mathrm{y}}, \boldsymbol{u}, \boldsymbol{c}} \quad & -\boldsymbol{p}_{\mathrm{d}}^{\mathrm{T}} \boldsymbol{u} + \boldsymbol{q}_{\mathrm{y}}^{\mathrm{T}} \boldsymbol{c} && \text{(12a)} \\ \mathrm{s.\,t.} \quad & \boldsymbol{p}_{\mathrm{r}}^{\mathrm{T}} \boldsymbol{u} = 1, && \text{(12b)} \\ & c_i \ge |\boldsymbol{b}_i^{\mathrm{T}} \boldsymbol{u}|, \quad i = 1, \dots, m, && \text{(12c)} \\ & \boldsymbol{q}_{\mathrm{y}} = \mathrm{diag}(\tilde{\boldsymbol{q}}_{\mathrm{y}}) \boldsymbol{t}, && \text{(12d)} \\ & \boldsymbol{t} \in \mathcal{T}(\alpha, \tilde{\boldsymbol{t}}). && \text{(12e)} \end{aligned}$$

Thus $\lambda_{\mathrm{min}}(\alpha, \tilde{\boldsymbol{x}})$ is obtained as the optimal value of this problem. Note that $\boldsymbol{t}$, $\boldsymbol{q}_{\mathrm{y}}$, $\boldsymbol{u}$, and $\boldsymbol{c}$ are the variables to be optimized. The worst scenario, $\boldsymbol{t}_{\mathrm{w}}$, is optimal for problem (12).

Remark 2.4. It follows from definition (10) of λ_{min} and $\mathcal{T}(0, \tilde{\boldsymbol{t}}) = \{\tilde{\boldsymbol{t}}\}$ that

$$\lambda_{\mathrm{min}}(0, \tilde{\boldsymbol{x}}) = \lambda^*(\tilde{\boldsymbol{x}}).$$

That is, the worst limit load factor at $\alpha = 0$ coincides with the nominal limit load factor. ■

Remark 2.5. The uncertainty set $\mathcal{T}(\alpha, \tilde{\boldsymbol{t}})$ consists of finite number of elements. For example, $|\mathcal{T}(1, \tilde{\boldsymbol{t}})| = m + 1$. Hence, the optimal solution of problem (12) for $\alpha = 1$ can be found by performing the conventional limit analysis, problem (8), for all $m + 1$ trusses included in $\mathcal{T}(1, \tilde{\boldsymbol{t}})$. However, since $|\mathcal{T}(\alpha, \tilde{\boldsymbol{t}})|$ is the sum of combinations of selecting α' truss members ($1 \le \alpha' \le \alpha$) from m members, it increases exponentially as α increases. Therefore, it is not acceptable to attempt to solve problem (8) by enumerating all the scenarios included in $\mathcal{T}(\alpha, \tilde{\boldsymbol{t}})$. This motivates us to explore an MILP reformulation of problem (8) in section 3. ■

Remark 2.6. Let $\mathcal{D}(\alpha, \tilde{\boldsymbol{t}})$ be the set of trusses which differ from $\tilde{\boldsymbol{t}}$ by removing exactly α members, i.e.,

$$\mathcal{D}(\alpha, \tilde{\boldsymbol{t}}) = \{\boldsymbol{t} \in \mathcal{T}(\alpha, \tilde{\boldsymbol{t}}) \mid \|\tilde{\boldsymbol{t}} - \tilde{\boldsymbol{t}}\|_1 = \min\{\alpha, \|\tilde{\boldsymbol{t}}\|_1\}\}, \quad \alpha \in \{0\} \cup \mathbb{N}.$$

This set, called the *deficiency set*, was introduced in Example 3 of [22]. Then we can show that (12e) can be replaced by

$$\boldsymbol{t} \in \mathcal{D}(\alpha, \tilde{\boldsymbol{t}}) \tag{13}$$

without changing the optimal value of problem (12). Since $\mathcal{D}(\alpha, \tilde{\boldsymbol{t}}) \subset \mathcal{T}(\alpha, \tilde{\boldsymbol{t}})$ ($\forall \alpha \in \mathbb{N}$), the practical computational effort can possibly be smaller by using (13) instead of (12e). However, we consider (12e) throughout the paper to make clear that α represents the magnitude of uncertainty, as discussed in section 2.1. The results in section 3 also hold true for (13). ■

2.4 Quantitative measure of robustness

For a general system possesses uncertainties, Ben-Haim [2] proposed a decision theory called the *information-gap theory*. The *robustness function* was introduced there as a quantitative measure of robustness. In this section, this concept can be applied to our problem in question naturally to evaluate robustness of a structure against structural deficiency.

In the info-gap theory, the uncertainty parameter α is considered unknown. Then $\mathcal{T}(\alpha, \tilde{\boldsymbol{t}})$ defined by (2) corresponds to the info-gap uncertainty model discussed in Example 6 of [22]. Suppose that the limit load factor is required not to be smaller than λ_{c}. We call λ_{c} the *critical performance*. Given a design of the truss $\tilde{\boldsymbol{x}}$ and a critical performance λ_{c}, the robustness function, denoted $\hat{\alpha}(\tilde{\boldsymbol{x}}, \lambda_{\mathrm{c}})$, is defined as the largest number of deficient members up to which the performance requirement is satisfied. By using the worst limit load factor defined by (10), the robustness function is given by

$$\hat{\alpha}(\tilde{\boldsymbol{x}}, \lambda_{\mathrm{c}}) = \max_{\alpha}\{\lambda_{\min}(\alpha, \tilde{\boldsymbol{x}}) \geq \lambda_{\mathrm{c}}\}. \tag{14}$$

We define $\hat{\alpha}(\tilde{\boldsymbol{x}}, \lambda_{\mathrm{c}}) = 0$ if $\lambda_{\min}(0, \tilde{\boldsymbol{x}}) < \lambda_{\mathrm{c}}$. Consider two different designs of a truss, say, $\boldsymbol{x}$ and $\boldsymbol{x}'$. If $\hat{\alpha}(\tilde{\boldsymbol{x}}, \lambda_{\mathrm{c}}) < \hat{\alpha}(\tilde{\boldsymbol{x}}', \lambda_{\mathrm{c}})$, then $\boldsymbol{x}'$ is considered more robust than $\boldsymbol{x}$ for the performance requirement λ_{c}, because $\boldsymbol{x}'$ allows that more members are absent without violating the performance requirement.

3 Mixed integer linear programming formulations

The worst scenario problem (12) is reduced to a tractable form in section 3.1. Section 3.2 discusses uncertainty in partial deficiency scenarios of structural components.

3.1 MILP formulation for worst scenario problem

In section 2.3, we saw that the worst scenario is obtained as the optimal solution of problem (12). It is worth of noting that this problem should be solved by an algorithm with guaranteed global convergence, because, obviously, a local (but not global) optimal solution is not the worst scenario. Unfortunately, it is difficult to find the global optimal solution of problem (12). This is because integrality constraints are involved in (12e) and the objective function is nonconvex due to the nonlinear term $\boldsymbol{q}_{\mathrm{y}}^{\mathrm{T}}\boldsymbol{c}$. These difficulties motivate us to reformulate problem (12) as an MILP problem, which can be solved globally with a branch-and-bound method or a branch-and-cut method, etc.

A key idea for this reduction is to rewrite the nonlinear term $q_{\mathrm{y}i}c_i$ by using a system of linear inequalities with integrality constraints as follows.

Proposition 3.1. *Let $M > 0$ be a sufficiently large constant. Then $(t_i, q_{\mathrm{y}i}, c_i, w_i)$ satisfies*

$$w_i = q_{\mathrm{y}i}c_i, \tag{15a}$$

$$q_{\mathrm{y}i} = \tilde{q}_{\mathrm{y}i}t_i, \tag{15b}$$

$$t_i \in \{0, 1\} \tag{15c}$$

if and only if (t_i, c_i, w_i) satisfies

$$M(1 - t_i) \geq |w_i - \tilde{q}_{\mathrm{y}i}c_i|, \tag{16a}$$

$$Mt_i \geq |w_i|, \tag{16b}$$

$$t_i \in \{0, 1\} \tag{16c}$$

and $q_{\mathrm{y}i}$ is defined by (15b).

Proof. We begin by observing that (15) is reduced to

$$w_i = \begin{cases} \tilde{q}_{\mathrm{y}i}c_i & \text{if } t_i = 1, \\ 0 & \text{if } t_i = 0. \end{cases} \tag{17}$$

We show that (16) is equivalent to (17).

Suppose that $t_i = 1$. Then (16a) is reduced to (17). This w_i satisfies (16b), which is reduced to $M \geq |w_i|$, because M is assumed to be sufficiently large. Alternatively, suppose that $t_i = 0$. Then (16b) is reduced to (17). This w_i and any c_i satisfy $M \geq |w_i - \tilde{q}_{\mathrm{y}}c_i|$, i.e., (16a). □

Note again that (15a) is a nonconvex constraint. In contrast, (16a) and (16b) are linear inequality constraints. Therefore, (16) is more tractable than (15).

As a consequence of Proposition 3.1, problem (12) can be rewritten equivalently as

$$\begin{aligned} \min_{\boldsymbol{t},\boldsymbol{u},\boldsymbol{c},\boldsymbol{w}} \quad & -\boldsymbol{p}_{\mathrm{d}}^{\mathrm{T}}\boldsymbol{u} + \sum_{i=1}^{m} w_i && && (18\mathrm{a}) \\ \mathrm{s.\,t.} \quad & \boldsymbol{p}_{\mathrm{r}}^{\mathrm{T}}\boldsymbol{u} = 1, && && (18\mathrm{b}) \\ & c_i \geq |\boldsymbol{b}_i^{\mathrm{T}}\boldsymbol{u}|, && i = 1, \dots, m, && (18\mathrm{c}) \\ & M(1 - t_i) \geq |w_i - \tilde{q}_{\mathrm{y}i}c_i|, && i = 1, \dots, m, && (18\mathrm{d}) \\ & Mt_i \geq |w_i|, && i = 1, \dots, m, && (18\mathrm{e}) \\ & \boldsymbol{t} \in \mathcal{T}(\alpha, \tilde{\boldsymbol{t}}). && && (18\mathrm{f}) \end{aligned}$$

It follows from (18c) that any feasible solution of problem (18) satisfies $c_i \geq 0$. Since $\tilde{q}_{\mathrm{y}i} > 0$, the inequality

$$\tilde{q}_{\mathrm{y}i}c_i \geq 0 \tag{19}$$

holds for any feasible solution. Moreover, as shown in the proof of Proposition 3.1, any feasible solution satisfies (17). Therefore, c_i and w_i satisfy

$$0 \leq w_i \leq \tilde{q}_{\mathrm{y}i} c_i. \tag{20}$$

Thus, we can add (20) as additional constraints to problem (18) without changing the optimal solution. On the other hand, (18d) includes the inequality

$$w_i - \tilde{q}_{\mathrm{y}i} c_i \leq M(1 - t_i),$$

while (18e) includes the inequality

$$w_i \geq -M t_i.$$

These two inequalities become redundant, when we add (20) as additional constraints. Consequently, (18d) and (18e) can be replaced by

$$\begin{aligned} & -M(1 - t_i) \leq w_i - \tilde{q}_{\mathrm{y}i} c_i \leq 0, \quad && i = 1, \dots, m, && \text{(21a)} \\ & 0 \leq w_i \leq M t_i, && i = 1, \dots, m && \text{(21b)} \end{aligned}$$

without changing the optimal solution.

The upshot of the discussion above is that (18d) and (18e) can be tightened as (21a) and (21b). Thus, problem (18) (and hence problem (12) also) is equivalent to the following problem:

$$\begin{aligned} \min_{\boldsymbol{t}, \boldsymbol{u}, \boldsymbol{c}, \boldsymbol{w}} \quad & -\boldsymbol{p}_{\mathrm{d}}^{\mathrm{T}} \boldsymbol{u} + \sum_{i=1}^{m} w_i && && \text{(22a)} \\ \mathrm{s.\,t.} \quad & \boldsymbol{p}_{\mathrm{r}}^{\mathrm{T}} \boldsymbol{u} = 1, && && \text{(22b)} \\ & -c_i \leq \boldsymbol{b}_i^{\mathrm{T}} \boldsymbol{u} \leq c_i, && i = 1, \dots, m, && \text{(22c)} \\ & -M(1 - t_i) \leq w_i - \tilde{q}_{\mathrm{y}i} c_i \leq 0, && i = 1, \dots, m, && \text{(22d)} \\ & 0 \leq w_i \leq M t_i, && i = 1, \dots, m, && \text{(22e)} \\ & t_i \leq \tilde{t}_i, && i = 1, \dots, m, && \text{(22f)} \\ & \sum_{i=1}^{m} (\tilde{t}_i - t_i) \leq \alpha, && && \text{(22g)} \\ & t_i \in \{0, 1\}, && i = 1, \dots, m. && \text{(22h)} \end{aligned}$$

This is the goal formulation which we solve for detecting the worst scenario in the plastic limit analysis. Note that definition (2) of $\mathcal{T}(\alpha, \tilde{\boldsymbol{t}})$ was substituted into (18f).

In problem (22), continuous variables are $\boldsymbol{u}$, $\boldsymbol{c}$, and $\boldsymbol{w}$, while binary variables are $\boldsymbol{t}$. All the constraints other than the integrality constraints are linear constraints. Thus, problem (22) is an MILP programming problem, and hence it can be solved globally by using, e.g., a branch-and-cut algorithm. Several software packages, e.g., CPLEX [17] and Gurobi Optimizer [15], are available for this purpose.

Remark 3.2. A big constant $M \gg 0$ is used in problem (22). It is known that such a "big-M" should not be chosen larger than necessary, because constraints including unnecessarily large M often slow down the solution process. Unfortunately, it is not easy to guess the smallest admissible value of M in advance. However, once the problem is solved, then we can check if the value of M was appropriate or not as follows. For $t_i = 1$, (22e) yields $w_i \le M$. This constraint should not become active at the optimal solution, because it is not involved in the original problem in (12). Similarly, (22d) with $t_i = 0$ yields

$$-M \le w_i - \tilde{q}_{\mathrm{y}i} c_i. \tag{23}$$

Since $c_i = |\boldsymbol{h}_i^{\mathrm{T}} \boldsymbol{u}|$ holds at the optimal solution of problem (12) and (22e) with $t_i = 0$ implies $w_i = 0$, (23) reads $\tilde{q}_{\mathrm{y}i} |\boldsymbol{h}_i^{\mathrm{T}} \boldsymbol{u}| \le M$. This constraint should be inactive at the optimal solution of problem (22). In short, if the optimal solution of problem (22), denoted $(\bar{\boldsymbol{t}}, \bar{\boldsymbol{u}}, \bar{\boldsymbol{c}}, \bar{\boldsymbol{w}})$, satisfies

$$\begin{aligned} &\bar{w}_i < M, && i = 1, \dots, m, \\ &\tilde{q}_{\mathrm{y}i} |\boldsymbol{h}_i^{\mathrm{T}} \bar{\boldsymbol{u}}| < M, && i = 1, \dots, m, \end{aligned}$$

then $(\bar{\boldsymbol{t}}, \bar{\boldsymbol{q}}_{\mathrm{y}}, \bar{\boldsymbol{u}}, \bar{\boldsymbol{c}})$ defined by $\bar{\boldsymbol{q}}_{\mathrm{y}} = \mathrm{diag}(\tilde{\boldsymbol{q}}_{\mathrm{y}}) \bar{\boldsymbol{t}}$ is correctly optimal for problem (12). ■

3.2 Partial deficiency model of structural components

In the preceding sections, we supposed that a damaged structural component is completely absent. Namely, the true value of the member cross-sectional area was assumed to be given as

$$x_i = \begin{cases} \tilde{x}_i & \text{if } t_i = 1, \\ 0 & \text{if } t_i = 0. \end{cases} \tag{24}$$

Such complete deficiency of structural components may not occur frequently in a real-life structure. Therefore, the worst scenario analysis based on this damage model might be rather pessimistic. In this section, we explore a damage model in which structural components are possibly diminishing in part.

Let $\rho \in [0, 1[$ be a constant representing the degree of damage. We assume that all members share same value of ρ. We use t_i, obeying the uncertainty model in (2), to indicate soundness of member i. Specifically, member i is intact if $t_i = 1$, while its cross-sectional area diminishes to $\rho \tilde{x}_i$ due to damage if $t_i = 0$. Since we are not worried about possible increase of member cross-sectional areas, we let $\rho < 1$. In short, the true value of the member cross-sectional area, x_i, is given by

$$\begin{aligned} x_i &= [t_i + \rho(1 - t_i)] \tilde{x}_i \\ &= \begin{cases} \tilde{x}_i & \text{if } t_i = 1, \\ \rho \tilde{x}_i & \text{if } t_i = 0. \end{cases} \end{aligned} \tag{25}$$

Note that this model reverts to (24) if $\rho = 0$. The modulus of the admissible axial force, $q_{\mathrm{y}i}$, is then written as

$$q_{\mathrm{y}i} = \sigma_{\mathrm{y}} x_i = [t_i + \rho(1 - t_i)] \tilde{q}_{\mathrm{y}i}. \tag{26}$$

If $\rho = 0$, then (26) certainly reverts to (4).

From (26), the internal plastic work of member i, denoted w_i, is related to the plastic member elongation c_i as

$$w_i = q_{\mathrm{y}i} c_i, \tag{27a}$$

$$q_{\mathrm{y}i} = [t_i + \rho(1 - t_i)]\tilde{q}_{\mathrm{y}i}, \tag{27b}$$

$$t_i \in \{0, 1\}. \tag{27c}$$

Since $c_i \geq 0$, $\tilde{q}_{\mathrm{y}i} > 0$, and $0 \leq \rho < 1$, (27) implies that w_i and $\tilde{q}_{\mathrm{y}i}$ satisfy

$$0 \leq w_i \leq \tilde{q}_{\mathrm{y}i} c_i. \tag{28}$$

In a manner similar to Proposition 3.1 (see also the discussion below Proposition 3.1), we can show that (27) and (28) can be rewritten equivalently as

$$-M(1 - t_i) \leq w_i - \tilde{q}_{\mathrm{y}i} c_i \leq 0, \tag{29a}$$

$$0 \leq w_i - \rho \tilde{q}_{\mathrm{y}i} c_i \leq M t_i, \tag{29b}$$

$$t_i \in \{0, 1\}, \tag{29c}$$

where M is a sufficiently large constant.

Consequently, the worst scenario problem for the partial deficient model of structural components can also be formulated as an MILP problem. Specifically, by replacing (22d) and (22e) in problem (22) by (29), we obtain the following MILP problem:

$$\begin{aligned}
\min_{\boldsymbol{t},\boldsymbol{u},\boldsymbol{c},\boldsymbol{w}} \quad & -\boldsymbol{p}_{\mathrm{d}}^{\mathrm{T}} \boldsymbol{u} + \sum_{i=1}^{m} w_i && && (30\mathrm{a}) \\
\mathrm{s.\,t.} \quad & \boldsymbol{p}_{\mathrm{r}}^{\mathrm{T}} \boldsymbol{u} = 1, && && (30\mathrm{b}) \\
& -c_i \leq \boldsymbol{b}_i^{\mathrm{T}} \boldsymbol{u} \leq c_i, && i = 1, \dots, m, && (30\mathrm{c}) \\
& -M(1 - t_i) \leq w_i - \tilde{q}_{\mathrm{y}i} c_i \leq 0, && i = 1, \dots, m, && (30\mathrm{d}) \\
& 0 \leq w_i - \rho \tilde{q}_{\mathrm{y}i} c_i \leq M t_i, && i = 1, \dots, m, && (30\mathrm{e}) \\
& t_i \leq \tilde{t}_i, && i = 1, \dots, m, && (30\mathrm{f}) \\
& \sum_{i=1}^{m} (\tilde{t}_i - t_i) \leq \alpha, && && (30\mathrm{g}) \\
& t_i \in \{0, 1\}, && i = 1, \dots, m. && (30\mathrm{h})
\end{aligned}$$

If $\rho = 0$, this problem certainly reverts to problem (22).

4 Numerical examples

The worst scenarios of two trusses are computed by solving problem (22). Computation was carried out on Core 2 Duo (2.26 GHz) with 4.0 GB RAM. The mixed integer linear programming problems were solved by using CPLEX Ver. 11.2 [17] with the default setting.

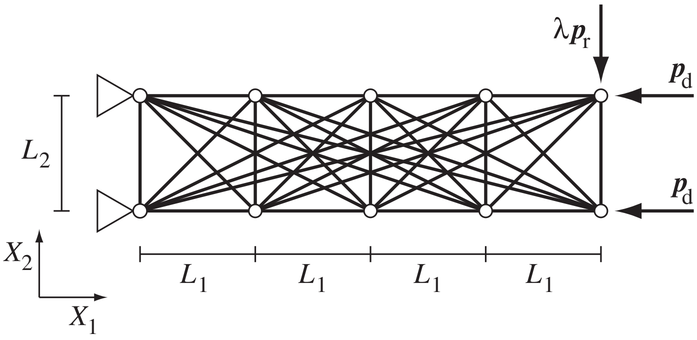

Figure 1: A 32-member plane truss.

Table 1: Limit load factors in the worst scenarios of the plane truss example.

α	$\lambda_{\min}(\alpha, \tilde{\boldsymbol{x}})$	
	$\rho = 0$	$\rho = 0.2$
0	10.0000	10.0000
1	8.7500	9.0000
2	7.5000	8.0000
3	6.0716	7.0000
4	2.2855	6.0000
5	$-\infty$	3.2704
6	$-\infty$	3.2704

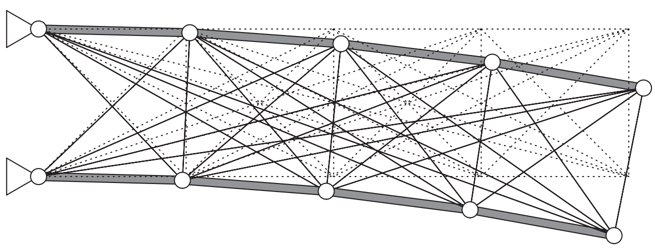

Figure 2: The collapse mode of the nominal structure of the plane truss example. The members represented by thick lines experience plastic deformations.

4.1 A plane truss example

Consider the plane truss in Figure 1, where $L_1 = L_2 = 1\,\mathrm{m}$. The truss consists of $m = 32$ members. The leftmost nodes are pin-supported, and hence the number of degrees of freedom of displacements is $d = 16$. The yield stress is $\sigma_{\rm y} = 200\,\mathrm{MPa}$ and the intact cross-sectional area of each member is $\tilde{x}_i = 1000\,\mathrm{mm}^2$. Therefore, $\tilde{q}_{{\rm y}i} = 200\,\mathrm{kN}$ ($i = 1, \dots, m$). As the constant load, $\boldsymbol{p}_{\rm d}$, suppose that an external force of $50\,\mathrm{kN}$ is applied at each of two rightmost nodes in the negative direction of the X_1-axis. As the proportionally increasing part, $\lambda \boldsymbol{p}_{\rm r}$, a force of $10\lambda\,\mathrm{kN}$ is applied at the upper rightmost node in the negative direction of the X_2-axis.

The limit load factor of the undeficient structure is $\lambda_{\min}(0, \tilde{\boldsymbol{x}}) = \lambda^*(\tilde{\boldsymbol{x}}) = 10.0000$. The collapse mode is illustrated in Figure 2, where the members undergoing plastic deformations are depicted by

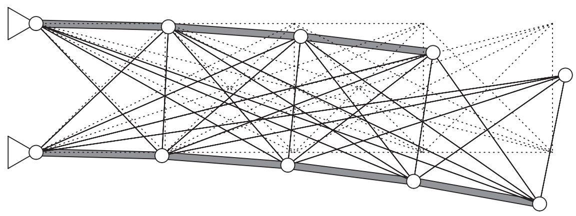

(a) $\alpha = 1$

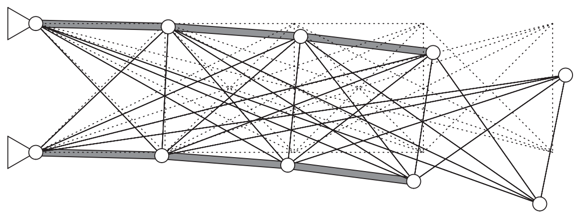

(b) $\alpha = 2$

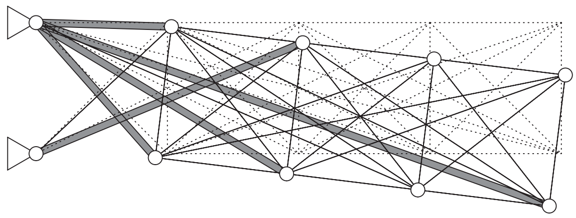

(c) $\alpha = 3$

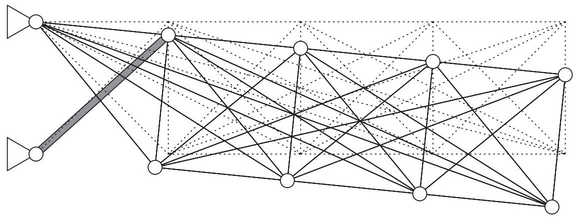

(d) $\alpha = 4$

Figure 3: Worst scenarios and collapse modes of the plane truss example ($\rho = 0$).

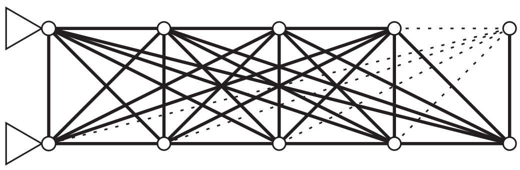

Figure 4: Worst scenario of the plane truss example for $\alpha = 5$ ($\rho = 0$).

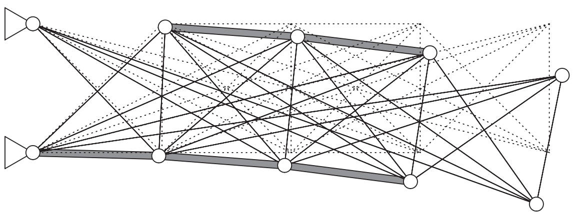

Figure 5: Worst scenario for $\alpha = 3$ when the two missing members in Figure 3(b) are specified to be absent ($\rho = 0$). The limit load factor of this scenario is 6.2500 ($> \lambda_{\min}(3, \tilde{\boldsymbol{x}})$).

thick lines.

4.1.1 Complete deficiency model

We first consider the complete deficiency model. That is, the member cross-sectional area is assumed to vanish if the corresponding member is damaged, as formulated in (24). This corresponds to the case of $\rho = 0$ in (25).

The worst scenarios for $\alpha = 1, \dots, 4$ are computed by solving problem (22). The obtained worst limit load factors, $\lambda_{\min}(\alpha, \tilde{\boldsymbol{x}})$, are listed in Table 1. The corresponding collapse modes are illustrated in Figure 3. Here, the yielding members are represented by thick lines and the deficient members are removed from the figures. Note that exactly α members are deficient in each case. Figure 4 illustrates one of deficiency scenarios for $\alpha = 5$, where the truss is kinematically indeterminate (or unstable) due to absence of five members. In this case, the force-balance equation, (6), has no

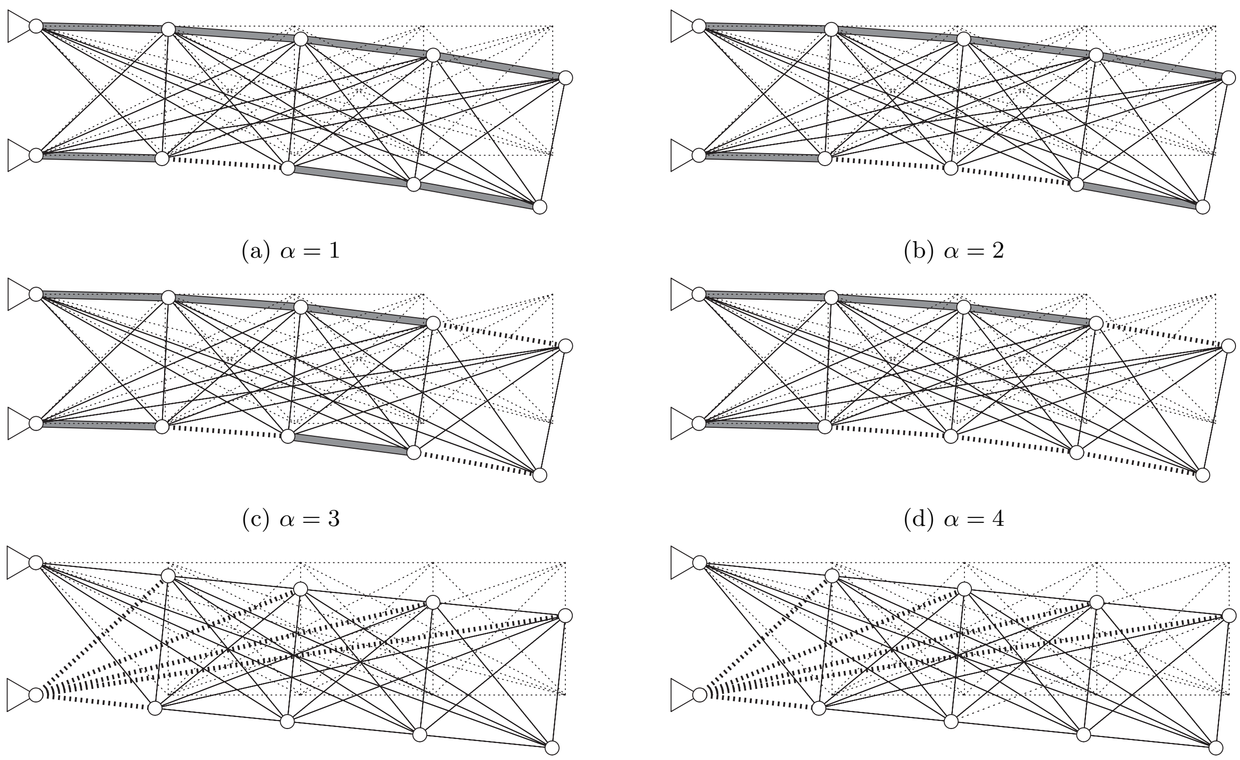

(a) $\alpha = 1$ (b) $\alpha = 2$

(c) $\alpha = 3$ (d) $\alpha = 4$

(e) $\alpha = 5$ (f) $\alpha = 6$

Figure 6: Worst scenarios and collapse modes of the plane truss example ($\rho = 0.2$).

solution, because external forces are applied to the unstable upper rightmost node. Therefore, from the discussion in Remark 2.3, we conclude $\lambda_{\min}(5, \tilde{\boldsymbol{x}}) = -\infty$.

In the worst scenarios collected in Figure 3, attention should be focused on the difference between the cases of $\alpha = 2$ and $\alpha = 3$. The two members missing in Figure 3(b) are undeficient in Figure 3(c). In other words, the set of missing members in Figure 3(c) is not a superset of the set of missing members in Figure 3(b). As a consequence, the yielding members in Figure 3(c) are different from those in Figure 3(b). For comparison, assume that the two members missing at $\alpha = 2$ are also absent in the case of $\alpha = 3$. In other words, we explore the worst set of three absent members when the set is restricted to a superset of the two members missing at $\alpha = 2$. The worst scenario in this case is shown in Figure 5. The corresponding limit load factor is 6.2500, which is larger than that of the scenario in Figure 3(c). Thus the worst scenario at $\alpha = 3$ cannot be obtained as a superset of the deficient members at $\alpha = 2$. This illustrates that “key” structural components, missing of which causes the worst structural degradation, depends on α.

4.1.2 Partial deficiency model

We now consider the partial deficiency model investigated in section 3.2. The member cross-sectional area is given by (25), where $\rho = 0.2$. Then the worst scenario is found by solving problem (30). The obtained worst scenario for $\alpha = 1, \dots, 6$ are shown in Figure 6. Here, deficient members are represented by dotted lines. Among them, thick dotted lines are yielding ones, while a member in Figure 6(f) represented by a thin dotted line is not deformed. Therefore, the collapse mode for $\alpha = 6$ is same as that for $\alpha = 5$. Note that the structures in all scenarios are stable, because no

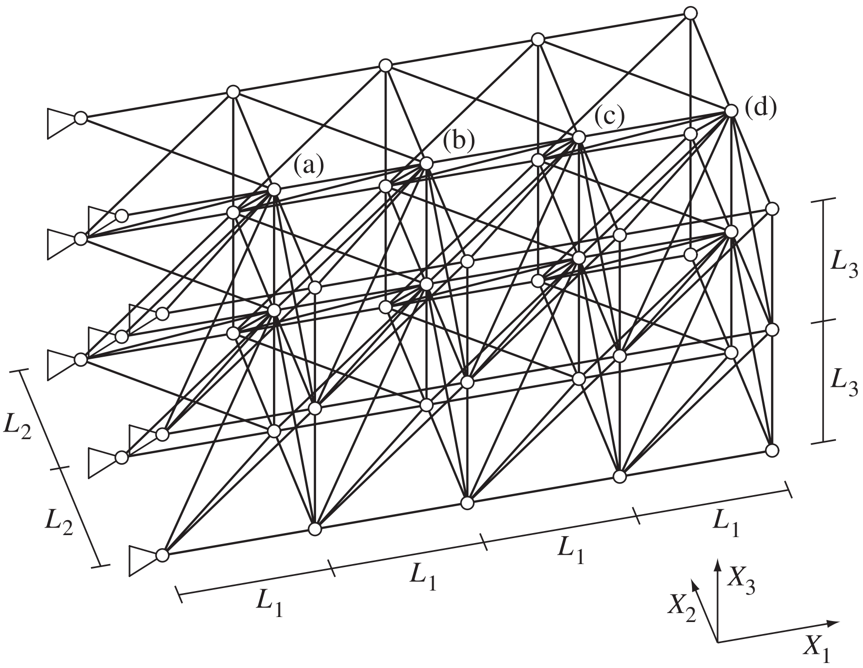

Figure 7: A 164-member space truss.

Table 2: Computational results of the space truss example.

α	$\lambda_{\min}(\alpha, \tilde{\boldsymbol{x}})$	CPU (s)	Nodes
0	140.7079	0.1	—
1	128.3622	0.7	68
2	115.1253	33.5	7,301
3	97.3447	570.4	89,925
4	79.2562	2,455.6	321,155
5	57.7350	2,872.7	677,656
6	0.0000	25.5	1,251

member is absent in the partial deficiency model. The locations of yield members for $\alpha = 5$ and $\alpha = 6$ are much different from those for $\alpha = 1, \dots, 4$. The limit load factors in the worst scenarios are listed in Table 1. For a given α, the worst limit load factor for $\alpha = 0.2$ is, naturally, larger than that for $\rho = 0$.

4.2 A space truss example

We next consider the space truss in Figure 7, where $L_1 = L_2 = L_3 = 1\,\mathrm{m}$. The truss consists of $m = 164$ members and is in a cuboidal shape. The nine leftmost nodes, depicted with triangles, are pin-supported, and hence the number of degrees of freedom of displacements is $d = 108$. The yield stress is $\sigma_{\mathrm{y}} = 200\,\mathrm{MPa}$ and the cross-sectional area of each undeficient member is $\tilde{x}_i = 500\,\mathrm{mm}^2$. Therefore, the modulus of the admissible axial force is $\tilde{q}_{\mathrm{y}i} = 100\,\mathrm{kN}$ for each $i = 1, \dots, m$. The constant part of the external load is set $\boldsymbol{p}_{\mathrm{d}} = \boldsymbol{0}$. As the parametrically increasing part, $\lambda \boldsymbol{p}_{\mathrm{r}}$, the

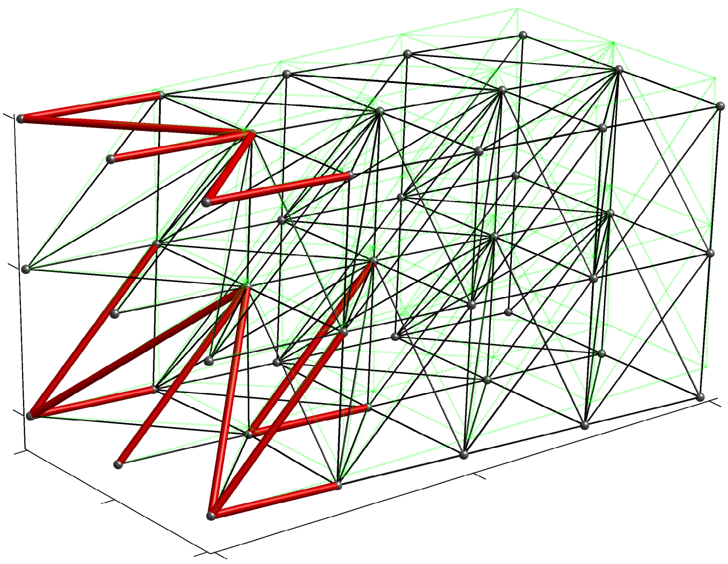

Figure 8: The collapse mode of the nominal structure of the space truss example. The members represented by thick lines experience plastic deformations.

following forces are applied at nodes (a)–(d) in Figure 7. Forces of $0.1\lambda\,\mathrm{kN}$ are applied at nodes (a)–(d) in the negative direction of the X_1-axis. Then, in the negative direction of the X_3-axis, forces of $0.5\lambda\,\mathrm{kN}$ are applied at nodes (a) and (b), while forces of $\lambda\,\mathrm{kN}$ are applied at nodes (c) and (d).

The limit load factor of the undeficient structure is $\lambda_{\min}(0, \tilde{\boldsymbol{x}}) = \lambda^*(\tilde{\boldsymbol{x}}) = 140.7079$. The corresponding collapse mode is shown in Figure 8.

We assume that damaged members have vanishing cross-sectional areas, i.e., (24). By solving the MILP problem (22), we find the worst scenarios for $\alpha = 1, \dots, 6$. The obtained deficiency scenarios, as well as the collapse modes, are shown in Figure 9. The absent members are depicted by dotted lines. It is observed that the collapse modes for $\alpha = 5$ and $\alpha = 6$ are qualitatively different from those for $\alpha = 0, 1, \dots, 4$. At the worst scenario for $\alpha = 6$, the truss becomes kinematically indeterminate. The limit load factors in these worst scenarios and the computational efforts are listed in Table 2. Here, "CPU" represents the computational time spent to solve problem (22) with CPLEX [17], and "Nodes" represents the number of visited nodes of the branch-and-bound tree. Note that more than 40 minutes are required for solving the problem with $\alpha = 5$. On the other hand, by definition, the number of feasible solutions of this problem, i.e., the number of scenarios in the uncertainty set, is

$$|\mathcal{T}(5, \tilde{\boldsymbol{x}})| = 1 + \sum_{\alpha=1}^{5} \binom{m}{\alpha} = 959{,}418{,}328.$$

Therefore, it is unviable to enumerate scenarios for finding the worst one.

As discussed in section 2.4, the worst limit load factor can be linked to a measure of robustness. Specifically, recall that the robustness function, $\hat{\alpha}(\tilde{\boldsymbol{x}}, \lambda_{\mathrm{c}})$, is defined by (14). From the results in Table 2, the variation of $\hat{\alpha}(\tilde{\boldsymbol{x}}, \lambda_{\mathrm{c}})$ with respect to λ_{c} is depicted as Figure 10. The trade-off relation between $\hat{\alpha}(\tilde{\boldsymbol{x}}, \lambda_{\mathrm{c}})$ and λ_{c} can be captured from this curve. Namely, the robustness cannot be improved (i.e., $\hat{\alpha}(\tilde{\boldsymbol{x}}, \lambda_{\mathrm{c}})$ cannot be larger) when the requirement of the performance becomes severer (i.e., λ_{c}

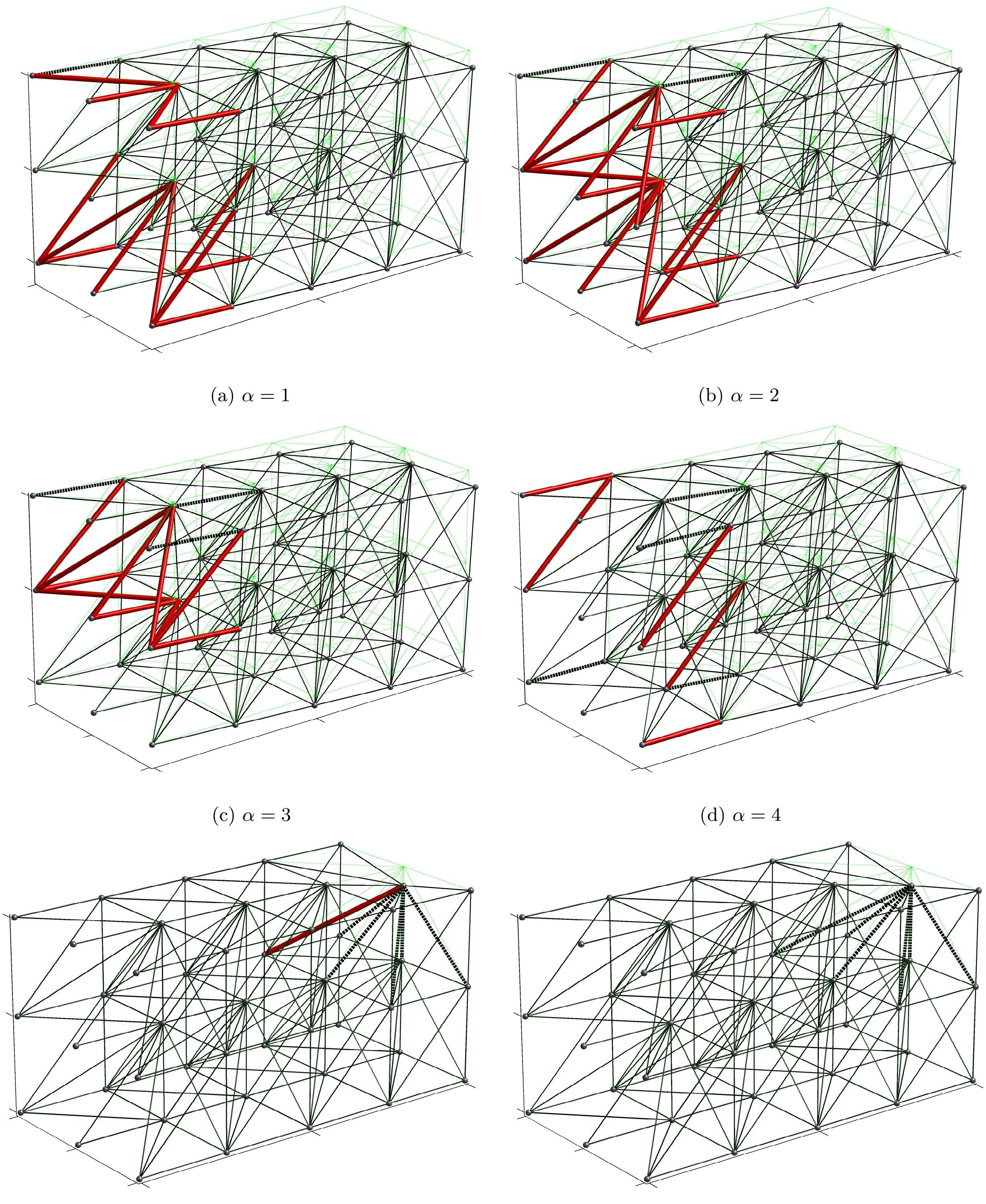

(a) $\alpha = 1$

(b) $\alpha = 2$

(c) $\alpha = 3$

(d) $\alpha = 4$

(e) $\alpha = 5$

(f) $\alpha = 6$

Figure 9: Worst scenarios and collapse modes of the space truss example.

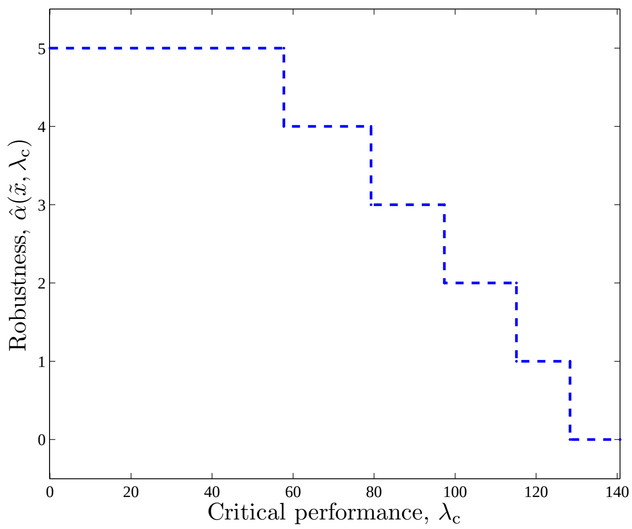

Figure 10: Trade-off relation between robustness and the critical performance for the space truss example.

becomes larger).

5 Concluding remarks

To evaluate the redundancy and the robustness of a structure, a key is to assess the amount of degradation of a structural performance when the structural system is subjected to uncertainty. Roughly speaking, a structure is considered more robust and/or redundant if it can maintain a specified performance requirement even when the structure suffers large uncertainty. Robust satisfaction of a performance constraint against the specified amount of uncertainty can be checked by finding the worst scenario. In this paper, we explored worst scenario detection in the plastic limit analysis of a truss when one or more structural components fail.

The worst scenario problem was clearly formulated as the minimization problem of the limit load factor under possible absent of the specified number of structural components. The set of absent components in the worst scenario can be viewed as a set of key elements in the truss, in the sense that absence of them causes the largest degradation of the limit load factor. For numerical solution of this optimization problem, an algorithm with guaranteed global convergence is required, because a local (but not global) optimal solution corresponds to more optimistic scenario than the true worst scenario. To enjoy existing global algorithms such as a branch-and-cut method, we reformulated the worst scenario problem as a mixed integer linear programming problem.

Discussion in this paper is restricted to degradation of the limit load factor of a truss. Other problems remain to be explored. For instance, a worst scenario problem of a frame structure against deficiency of columns in progressive collapse is important from a practical point of view [11, 18, 23, 32]. Also, implications of the worst scenario in designing a structure can be explored.

Acknowledgments

This work is supported in part by a Grant-in-Aid for Scientific Research from the Ministry of Education, Culture, Sports, Science and Technology of Japan.

References

[1] Alefeld, G., Mayer, G.: Interval analysis: theory and applications. *Journal of Computational and Applied Mathematics*, **121**, 421–464 (2000).

[2] Ben-Haim, Y.: *Information-gap Decision Theory: Decisions under Severe Uncertainty (2nd ed.)*. Academic Press, London (2006).

[3] Ben-Haim, Y., Elishakoff, I.: *Convex Models of Uncertainty in Applied Mechanics*. Elsevier, New York (1990).

[4] Ben-Tal, A., El Ghaoui, L., Nemirovski, A.: *Robust Optimization*. Princeton University Press, Princeton (2009).

[5] Chen, S., Lian, H., Yang, X.: Interval static displacement analysis for structures with interval parameters. *International Journal for Numerical Methods in Engineering*, **53**, 393–407 (2002).

[6] Degrauwe, D., Lombaert, G., De Roeck, G.: Improving interval analysis in finite element calculations by means of affine arithmetic. *Computers and Structures*, **88**, 247–254 (2010).

[7] Elishakoff, I., Ohsaki, M.: *Optimization and Anti-Optimization of Structures under Uncertainties*. Imperial College Press, London (2010).

[8] Feng, Y.S., Moses, F.: Optimum design, redundancy and reliability of structural systems. *Computers and Structures*, **24**, 239–251 (1986).

[9] Frangopol, D.M., Curley, J.P.: Effects of damage and redundancy on structural reliability. *Journal of Structural Engineering (ASCE)*, **113**, 1533–1549 (1987).

[10] Ganzerli, S., Pantelides, C.P.: Optimum structural design via convex model superposition. *Computers and Structures*, **74**, 639–647 (1998).

[11] Gerasimidis, S., Baniotopoulos, C.C.: Steel moment frames column loss analysis: the influence of time step size. *Journal of Constructional Steel Research*, **67**, 557–564 (2011).

[12] Guo, X., Bai, W., Zhang, W.: Extreme structural response analysis of truss structures under material uncertainty via linear mixed 0–1 programming. *International Journal for Numerical Methods in Engineering*, **76**, 253–277 (2008).

[13] Guo, X., Bai, W., Zhang, W.: Confidence extremal structural response analysis of truss structures under static load uncertainty via SDP relaxation. *Computers and Structures*, **87**, 246–253 (2009).

[14] Guo, X., Bai, W., Zhang, W., Gao, X.: Confidence structural robust design and optimization under stiffness and load uncertainties. *Computer Methods in Applied Mechanics and Engineering*, **198**, 3378–3399 (2009).

[15] Gurobi Optimization, Inc.: *Gurobi Optimizer Reference Manual*. `http://www.gurobi.com/`.

[16] Hlaváček, I., Chleboun, J., Babuška, I.: *Uncertain Input Data Problems and the Worst Scenario Method*. Elsevier, Amsterdam (2004).

[17] IBM ILOG: *User's Manual for CPLEX*. `http://www.ilog.com`.

[18] Izzuddin, B.A., Vlassis, A.G., Elghazouli, A.Y., Nethercot, D.A.: Progressive collapse of multi-storey buildings due to sudden column loss—Part I: simplified assessment framework. *Engineering Structures*, **30**, 1308–1318 (2008).

[19] Kanno, Y., Takewaki, I.: Confidence ellipsoids for static response of trusses with load and structural uncertainties. *Computer Methods in Applied Mechanics and Engineering*, **196**, 393–403 (2006).

[20] Kanno, Y., Takewaki, I.: Worst-case plastic limit analysis of trusses under uncertain loads via mixed 0–1 programming. *Journal of Mechanics of Materials and Structures*, **2**, 245–273 (2007).

[21] Kanno, Y., Takewaki, I.: Semidefinite programming for uncertain linear equations in static analysis of structures. *Computer Methods in Applied Mechanics and Engineering*, **198**, 102–115 (2008).

[22] Kanno, Y., Ben-Haim, Y.: Redundancy and robustness, or, when is redundancy redundant? *Journal of Structural Engineering (ASCE)*, to appear. The preprint is available at `http://www.technion.ac.il/yakov/rr09.pdf`.

[23] Kim, J., Park, J.-H., Lee, T.H.: Sensitivity analysis of steel buildings subjected to column losss. *Engineering Structures*, **33**, 421–432 (2011).

[24] McWilliam, S.: Anti-optimization of uncertain structures using interval analysis. *Computers and Structures*, **79**, 421–430 (2001).

[25] Moens, D., Vandepitte, D.: A survey of non-probabilistic uncertainty treatment in finite element analysis. *Computer Methods in Applied Mechanics and Engineering*, **194**, 1257–1555 (2005).

[26] Moens, D., Vandepitte, D.: Interval sensitivity theory and its application to frequency response envelope analysis of uncertain structures. *Computer Methods in Applied Mechanics and Engineering*, **196**, 2486–2496 (2007).

[27] Neumaier, A.: *Interval Methods for Systems of Equations*. Cambridge University Press, Cambridge (1990).

[28] Ohi, K., Ito, T., Li, Z.-L: Sensitivity on load carrying capacity of frames to member disappearance. *Proceedings of Council on Tall Building and Urban Habitat (CTBUH) Seoul Conference—Tall Buildings in Historical Cities: Culture & Technology for Sustainable Cities*, Seoul (2004).

[29] Pantelides, C.P., Ganzerli, S.: Design of trusses under uncertain loads using convex models. *Journal of Structural Engineering (ASCE)*, **124**, 318–329 (1998).

[30] Qiu, Z., Elishakoff, I.: Antioptimization of structures with large uncertain-but-non-random parameters via interval analysis. *Computer Methods in Applied Mechanics and Engineering*, **152**, 361–372 (1998).

[31] Schafer, B.W., Bajpai, P.: Stability degradation and redundancy in damaged structures. *Engineering Structures*, **27**, 1642–1651 (2005).

[32] Wada, A., Ohi, K., Suzuki, H., Sakumoto, Y., Fushimi, M., Kamura, H., Murakami, Y., Sasaki, M. Fujiwara, K.: Study of redundancy of high-rise building due to the effect of heat and loss of vertical structural members. *Proceedings of the 36th Joint Meeting Panel on Wind and Seismic Effects* (2004).

[33] Zhang, X.-M., Ding, H.: Design optimization for dynamic response of vibration mechanical system with uncertain parameters using convex model . *Journal of Sound and Vibration*, **318**, 406–415 (2008).